

This is the accepted manuscript made available via CHORUS. The article has been published as:

Origin of the magnetization and compensation temperature in rare-earth orthoferrites and orthochromates

Hong Jian Zhao, Jorge Íñiguez, Xiang Ming Chen, and L. Bellaiche

Phys. Rev. B **93**, 014417 — Published 12 January 2016

DOI: [10.1103/PhysRevB.93.014417](https://doi.org/10.1103/PhysRevB.93.014417)

Origin of the magnetization and compensation temperature in rare-earth orthoferrites and orthochromates

Hong Jian Zhao^{1,2}, Jorge Íñiguez^{3,4}, Xiang Ming Chen¹, and L. Bellaiche²

¹*Laboratory of Dielectric Materials, Department of Materials Science and Engineering, Zhejiang University, Hangzhou 310027, China*

²*Physics Department and Institute for Nanoscience and Engineering, University of Arkansas, Fayetteville, Arkansas 72701, USA*

³*Materials Research and Technology Department, Luxembourg Institute of Science and Technology (LIST),*

5 avenue des Hauts-Fourneaux, L-4362 Esch/Alzette, Luxembourg

⁴*Institut de Ciència de Materials de Barcelona (ICMAB-CSIC), Campus UAB, 08193 Bellaterra, Spain*

We consider orthoferrite and orthochromite perovskites with the formula RMO_3 , where R is a lanthanide and M is Fe or Cr. We identify an atomistic interaction that couples the magnetic moments of the R and M cations with the oxygen octahedral rotations characterizing these crystals. We show that this interaction results in an *effective magnetic field* acting on the R atoms, which in turn explains several intriguing features of these compounds, such as the existence (or absence) of a net magnetization associated to the R sublattice, its crystallographic direction, etc. Further, considered together with the couplings described by Bellaiche *et al.* [J. Phys.: Condens. Matt. **24**, 312201 (2012)], this interaction explains why some RMO_3 compounds display a *compensation temperature* at which the magnetization cancels and changes sign, while others do not.

PACS numbers: 75.25.-j, 75.10.-b, 75.47.Lx

I. INTRODUCTION

$RFeO_3$ and $RCrO_3$ perovskites, where R is a rare-earth atom of the lanthanide series, are called orthoferrites and orthochromates, respectively, because their crystal structure adopts the orthorhombic $Pbnm$ space group. These compounds have been studied for about 50 years, mostly because of their striking magnetic properties.^{1,2} Today, they are regaining interest because of their possible application in devices exploiting fast spin dynamics,^{3–7} and because some of them have recently been shown to exhibit a spontaneous electric polarization, which makes them multiferroic.^{3,4,8–10} Surprisingly, despite the flurry of activities devoted to these compounds, some of their key features remain poorly understood.

For example, it is known that, at low temperatures, the R sublattice can display a weak magnetization. This effect is believed to be the result of interactions between the $4f$ electrons of the R ions and the $3d$ electrons of the M transition metal ($M = \text{Fe, Cr}$), where the M spins would create an *effective magnetic field* acting on the R sublattice.^{11,12} However, the precise origin of this magnetization and effective magnetic field is unclear. Some argue that it is induced by the weak magnetization of the Fe/Cr sublattice.¹³ Others propose that it involves all the possible magnetic orderings (i.e., ferromagnetism, as well as G-, A- and C-types of antiferromagnetism) of this Fe/Cr sublattice.¹⁴ We are also still missing a discussion on how the peculiarities of the $Pbnm$ crystal structure – i.e., in-phase and antiphase oxygen octahedral tiltings and antiferroelectricity^{15,16} – may also affect the occurrence and nature of this effective magnetic field. This possibility is especially obvious when one notes that the magnetic ordering of the B -sublattice

of ABO_3 perovskites has been shown to depend on the octahedral tilting pattern,¹⁷ or that antiferroelectricity has been predicted to mediate magnetoelectric switching (i.e., reversal of the magnetic order parameter by application of electric field) in some perovskites.¹⁸

Another important, related property of these materials is the so-called *compensation temperature* at which the net magnetization (which arises from both the R and M cations) vanishes. In fact, some $RFeO_3$ and $RCrO_3$ compounds exhibit such a compensation temperature, while others do not.¹ The microscopic reason behind such difference remains to be elucidated. One may wonder if the presence of a compensation temperature might be related to the effective magnetic field mentioned above, which would align the R spins antiparallel to the Fe/Cr spins in the compounds presenting such a crossover.

Here we resolve all the aforementioned issues by identifying a previously overlooked microscopic coupling that explains the origin and nature of the effective magnetic field acting on the R ions. Such a field involves cross-products between vectors representing the antiferromagnetic order of the Fe/Cr spins and vectors characterizing oxygen octahedral tiltings. The effective field is proportional to a material-dependent constant, whose sign controls the existence or not of a compensation temperature.

II. METHODS

While most of this work is analytical, we also ran some simulations to illustrate some of points of the discussion. In particular, we employed the Vienna *ab-initio* Simulation Package (VASP), within the framework of the projected augmented wave (PAW) method,¹⁹ in order to

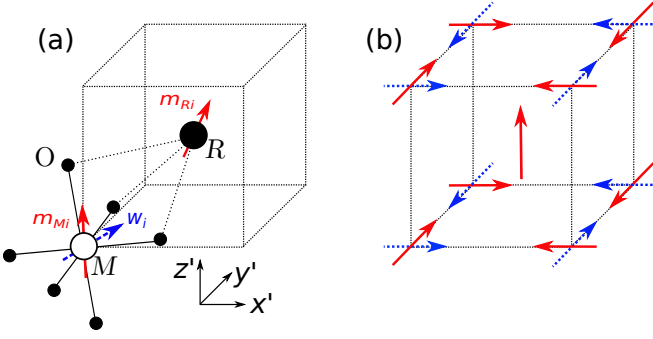


FIG. 1: Sketch of the 5-atom RMO_3 perovskite cell as described in the text. In panel (a), the most important R - O - M paths for magnetic interactions are marked for shown pair of R and M atoms. Panel (b) sketches all the $m_{Ri,z}$, $m_{Milmn,\beta}$, $\omega_{ilmn,\gamma}$ interactions for which \mathbf{m}_R is along z' and which are included in the term of Eq. (1). The invariance with respect to the full cubic symmetry (excepting operations that change the orientation of \mathbf{m}_R) is apparent.

simulate properties of the $GdFeO_3$ material. We used the Hubbard-corrected generalized gradient approximation (GGA+ U) method²⁰ with the Perdew and Wang parameterization.²¹ The Hubbard on-site Coulomb interaction U is chosen to be 4.0 eV and 3.0 eV for Gd and Fe, respectively, as consistent with previous works (see, e.g., Ref. 22). The valence electronic configurations of Gd, Fe and O are $4f^7 5s^2 5p^6 5d^1 6s^2$, $3d^7 4s^1$, and $2s^2 2p^4$, respectively; note that we allow the Gd ions to be spin-polarized since the $4f$ electrons are considered explicitly in the simulations. The energy cutoff is selected to be 500 eV, and the chosen Monkhorst-Pack k -point mesh (for the 20-atom orthorhombic cell) is $6 \times 6 \times 4$. Spin-orbit coupling and non-collinear magnetism are both included in the present computations.

III. RESULTS AND DISCUSSION

A. Magneto-structural couplings

Let us start by recalling which precise types of magnetic ordering of the R sublattice are known to be induced by the magnetic arrangements of the B spins in orthoferrites and orthochromites.¹⁴ Such orderings are indicated in Table I, using Bertaut's notation²³ for which the x , y , and z indices refer to the a , b , and c axes of the conventional cell of the $Pbnm$ structure. The A, C, and G symbols refer to the A-, C-, and G-type antiferromagnetic (AFM) arrangements, while F denotes the ferromagnetic one; all these refer to the Fe/Cr sublattice. Similar notations, but with the addition of a R superscript, are adopted for the magnetic orderings of the rare-earth spins. The magnetic states in Table I are the so-called Γ_1 , Γ_2 , Γ_3 , and Γ_4 spin configurations;^{14,23} all of them exhibit a magnetization of the R sublattice except Γ_1 , which presents a C-AFM component along the

z axis.

Let us now introduce the antiferrodistortive (AFD) pseudo-vector ω_i that characterizes the tilting of the oxygen octahedron centered at M -site i in the perovskite lattice. The direction of ω_i indicates the axis about which the octahedron rotates, while its magnitude gives the rotation angle.²⁴ We also adopt the following definitions: (i) \mathbf{m}_{Ri} is the magnetic dipole associated to the R cation at the 5-atom cell i , using the convention that the R and M cations of our RMO_3 structure are, respectively, at the center and corners of the 5-atom perovskite cell. (ii) The M -site i can be reached from the R -site i by a translation of $-a_{lat}/2(\mathbf{x}' + \mathbf{y}' + \mathbf{z}')$, where a_{lat} is the lattice constant of the 5-atom cubic cell. Here, \mathbf{x}' , \mathbf{y}' and \mathbf{z}' are the pseudo-cubic $[100]$, $[010]$, and $[001]$ directions, respectively. (The a , b , and c axes defined by the $Pbnm$ conventional cell lie along the pseudo-cubic $[\bar{1}10]$, $[110]$, and $[001]$ directions, respectively.) (iii) \mathbf{m}_{Milmn} is the magnetic moment of the M ion located at the cell that can be reached from cell i by following the lattice vector $a_{lat}(l\mathbf{x}' + m\mathbf{y}' + n\mathbf{z}')$, where l , m , and n are integers; (iv) ω_{ilmn} gives us the rotation of the octahedra centered at that same M ion. Note that $\mathbf{m}_{M,i000} = \mathbf{m}_{M,i}$ and $\omega_{i000} = \omega_i$.

As it is well-known, the O_6 rotations have a large effect on the coupling of M -spins at neighboring cells, an effect thoroughly studied in the literature on magnetic perovskites. Then, as sketched in Fig. 1(a), we can expect the octahedral tilts to affect the magnetic coupling between M and R spins as well, as such rotations modify the M - O - R interaction paths. We thus tackled the task of identifying the simplest atomistic interactions that couple neighboring \mathbf{m}_{Ri} and \mathbf{m}_{Mi} magnetic moments and the corresponding M -centered octahedral rotation ω_i .

In particular, we considered all possible trilinear terms coupling such variables, to identify which ones are allowed by symmetry. (We request invariance under the transformations of the full cubic group, as we want to study how the AFD modes – which lower the symmetry to orthorhombic – affect the magnetic couplings. Figure 1(b) shows a collection of trilinear couplings entering a symmetry invariant.) Then, from the symmetry-allowed couplings, we retained those that give a non-zero effect for the tilting patterns occurring in orthofer-

TABLE I: Magnetic orders of the M spins (the first column shows their labels, the second one gives the details of the spin arrangement; see text) that favor a certain magnetic order of the R spins (specified in the third column). This is derived by symmetry arguments in Ref. 23, assuming an orthorhombic atomic structure.

Mag. state	M spins	R spins
Γ_1	(A_x, G_y, C_z)	$(0, 0, C_z^R)$
Γ_2	(F_x, C_y, G_z)	$(F_x^R, C_y^R, 0)$
Γ_3	(C_x, F_y, A_z)	$(C_x^R, F_y^R, 0)$
Γ_4	(G_x, A_y, F_z)	$(0, 0, F_z^R)$

rites and orthochromites. The analysis of the results allowed us to identify (for the first time, to the best of our knowledge) the key interaction discussed in the following.

B. Magnetization of the R sublattice

This coupling is:

$$\Delta E_A = K_A \sum_i \sum_{lmn} \sum_{\alpha\beta\gamma} \epsilon_{\alpha\beta\gamma} m_{Ri,\alpha} m_{Milmn,\beta} \omega_{ilmn,\gamma}, \quad (1)$$

where α , β , and γ denote the spatial components of the corresponding vectors in the pseudo-cubic basis. The sum over i runs over all the 5-atom cells of the perovskite structure; the sums over l , m , and n run over 0 and 1; K_A is a material-dependent constant. $\epsilon_{\alpha\beta\gamma}$ is the Levi-Civita symbol, i.e., it equals 1 when the ordered triad $\alpha\beta\gamma$ forms a right-handed system, -1 when left-handed, and 0 when there are repeated indexes.

Interestingly, one can demonstrate that the ΔE_A coupling energy does not vanish only if the magnetic ordering of the M sublattice and the oxygen octahedral tiltings are associated with the same k -point of the first Brillouin zone of the ideal cubic perovskite structure. Such a condition is satisfied in only two cases, dictated by the particular tilting pattern of these materials. In the first one, the M -spins order in a G-type AFM fashion and the tilting occurs in antiphase; both spin arrangement and O_6 tilting are thus associated with the R -point of the first Brillouin zone, where $\mathbf{q}_R = 2\pi/a_{\text{lat}}(1/2, 1/2, 1/2)$. In the second case, the M spins adopt a C-type order and the oxygen tilt in phase, both patterns being characterized with the M -point where $\mathbf{q}_M = 2\pi/a_{\text{lat}}(1/2, 1/2, 0)$.

In the first case mentioned, we have $\mathbf{m}_{Mi} = (-1)^{n_{x'}(i)+n_{y'}(i)+n_{z'}(i)} \mathbf{G}$ and $\omega_i = (-1)^{n_{x'}(i)+n_{y'}(i)+n_{z'}(i)} \omega_R$, where \mathbf{G} characterizes the G-type AFM order of the M sublattice, ω_R is a vector quantifying the long-range antiphase tilting of the oxygen octahedra, and $n_{x'}(i)$, $n_{y'}(i)$, and $n_{z'}(i)$ are integers indexing the M -site i . (More precisely, site i is centered at $a_{\text{lat}}(n_{x'}(i)\mathbf{x}' + n_{y'}(i)\mathbf{y}' + n_{z'}(i)\mathbf{z}')$.) The second case corresponds to $\mathbf{m}_{Mi} = (-1)^{n_{x'}(i)+n_{y'}(i)} \mathbf{C}$ and $\omega_i = (-1)^{n_{x'}(i)+n_{y'}(i)} \omega_M$, where \mathbf{C} characterizes a possible C-type AFM component of the M spins and ω_M quantifies the in-phase oxygen octahedral tilting in the orthorhombic phase. It is also straightforward to show that, for these two cases, the only simple R -spin arrangement that renders a non-zero ΔE_A is the ferromagnetic one, which we denote by \mathbf{F}^R . Hence, we can simplify Eq. (1) to:

$$\Delta E_A = -8NK_A(\omega_R \times \mathbf{G} + \omega_M \times \mathbf{C}) \cdot \mathbf{F}^R. \quad (2)$$

To check the validity of Eq. (2) and its connection to the results of Table I, one simply needs to recall that the $Pbnm$ structure is characterized by an ω_R vector parallel to the y axis, while ω_M lies along the z axis (as

consistent with its $a^-a^-c^+$ representation in the notation introduced by Glazer²⁵). As a result, Eq. (2) tells us that the Γ_1 arrangement cannot have a magnetization associated to the R spins, because ω_R is collinear to \mathbf{G} , as is also the case of ω_M and \mathbf{C} . In contrast, Eq. (2) predicts the presence of a non-zero \mathbf{F}^R along the x or z axis when \mathbf{G} is along the z or x axis, respectively, as a result of the the first coupling term involving ω_R . These cases correspond precisely to the Γ_2 and Γ_4 spin configurations, respectively. Interestingly, the rare-earth magnetization of the Γ_3 state can instead be understood thanks to the second term in Eq. (2). Indeed, ω_M is along z and \mathbf{C} is parallel to x in this case, which results in \mathbf{F}^R along y . Equation (2) therefore explains in a straightforward way all the known facts about the magnetization of the R ions as induced by the M spins; that is, it explains its existence or absence, as well as its precise orientation.

It is also important to realize that our theory reveals that it is the G-type and/or C-type AFM component of the M sublattice, rather than its weak ferromagnetism (as proposed in Ref. 13), what drives the occurrence of a weak rare-earth magnetization. Further, the coupling in Eq. (2) renders a picture in which the magnetic ordering of the M spins and the oxygen octahedral tilting *work together* to create an effective magnetic field, $\mathbf{B}_{\text{eff}}^R$, acting on the rare-earth sublattice and given by

$$\mathbf{B}_{\text{eff}}^R \sim 8K_A(\omega_R \times \mathbf{G} + \omega_M \times \mathbf{C}). \quad (3)$$

C. Compensation temperature

It is well-known that, in some $R\text{FeO}_3$ and $R\text{CrO}_3$ materials (such as NdFeO_3 ,²⁷ SmFeO_3 ,^{28,29} EmFeO_3 ,²⁶ CeCrO_3 ,³⁰ GdCrO_3 ,^{10,31,32} TmCrO_3 ,^{10,31,33,34} and YbCrO_3 ,^{31,33,35}) the net magnetization vanishes at a specific *compensation* temperature, T_{comp} . This effect has been attributed to the fact that, below a certain temperature, the R ions acquire a magnetization that is opposite to that of the Fe/Cr sublattice and grows faster than the one of the B ions when further decreasing the temperature,^{26,27} as suggested by the relatively large paramagnetic susceptibility of the R spins.^{11,12} The two magnetizations cancel each other at T_{comp} , and further decreasing the temperature leads to a reversal of the magnetization sign, as the ground state magnetization of the R sublattice is larger than that of the M sublattice. Such an interpretation has recently received first-principles support²⁷ in the case of NdFeO_3 , which has the Γ_2 spin structure and is known to present a compensation temperature and magnetization reversal; the 0 K calculations yield a x -oriented magnetization of $-0.062 \mu_B$ per formula unit (fu) for the Nd sublattice, and of $+0.015 \mu_B/\text{fu}$ for the Fe ions.

On the other hand, other $R\text{FeO}_3$ and $R\text{CrO}_3$ materials do not display any compensation temperature, including TmFeO_3 ,³⁶ EuCrO_3 ,³⁷ DyCrO_3 ,³¹ HoCrO_3 ,^{31,33} ErCrO_3 ,^{31,33} and LuCrO_3 .³³ This absence may have two

different origins: either the magnetization of the R ions is again antiparallel to that of the Fe/Cr ions *but* \mathbf{F}^R is always smaller in magnitude than \mathbf{F} ; or, alternatively, \mathbf{F}^R is now parallel to \mathbf{F} . To check the latter possibility, we decided to perform first-principles computations of the Γ_4 spin configuration of GdFeO_3 , a material for which no compensation temperature has been reported,¹ within its $Pbnm$ crystal structure. Our 0 K calculations predict a magnetization of $+0.011 \mu_B/\text{fu}$ cell for the Gd ions and of $+0.023 \mu_B/\text{fu}$ cell for the Fe ions, both lying along $+z$. In other words, they confirm that the magnetizations of the Gd and Fe ions are parallel to each other, as consistent with the fact that GdFeO_3 displays no compensation temperature.

Let us try to understand why the weak magnetizations of the R and M ions can be either parallel or antiparallel to each other in different compounds. For that, we recall that Refs. 17,39 introduced an atomistic energetic term that affects the magnetic ordering of the M spins:

$$\Delta E_B = K_B \sum_i \sum_{j(i)} (\boldsymbol{\omega}_i - \boldsymbol{\omega}_j) \cdot (\mathbf{m}_{Mi} \times \mathbf{m}_{Mj}), \quad (4)$$

where i runs over all the M ions of the perovskite structure while j runs only over the M ions that are first-nearest neighbors of i . K_B is a material-dependent parameter. Equation (4) can be considered as a particular case of the Dzyaloshinsky-Moriya interaction^{40,41} – which is given by $\mathbf{D}' \cdot (\mathbf{m}_i \times \mathbf{m}_j)$ – in which \mathbf{D}' is proportional to the difference between the octahedral rotations at sites i and j . Reference 17 further demonstrated that Eq. (4) leads to the following couplings between long-range structural and magnetic order parameters

$$\begin{aligned} \Delta E_B = & 24NK_B(\boldsymbol{\omega}_R \times \mathbf{G}) \cdot \mathbf{F} + 16NK_B(\boldsymbol{\omega}_M \times \mathbf{C}) \cdot \mathbf{F} \\ & + 16NK_B(\boldsymbol{\omega}_M \times \mathbf{G}) \cdot \mathbf{A} + 8NK_B(\boldsymbol{\omega}_R \times \mathbf{C}) \cdot \mathbf{A}. \end{aligned} \quad (5)$$

As detailed in Ref. 17 and in the footnote³⁸, Eq. (5) can reproduce the coupled magnetic orderings known to be adopted by the B sublattice in ABO_3 perovskites, including those in Table I. The first two terms of Eq. (5) can also be interpreted as indicating that a magnetization can occur in the B -sublattice as a result of an effective magnetic field, \mathbf{B}_{eff} , given by

$$\mathbf{B}_{\text{eff}} \sim -24K_B(\boldsymbol{\omega}_R \times \mathbf{G}) - 16K_B(\boldsymbol{\omega}_M \times \mathbf{C}). \quad (6)$$

This magnetic field experienced by the B (or M) sublattice has a similar form and the same origin as the one of Eq. (3) acting on the R (or A) sublattice, as both depend on the cross products $\boldsymbol{\omega}_R \times \mathbf{G}$ and $\boldsymbol{\omega}_M \times \mathbf{C}$. However, these two fields also involve two different material-dependent constants, namely K_B for \mathbf{B}_{eff} and K_A for $\mathbf{B}_{\text{eff}}^R$. As a result, these fields, and thus the induced M - and R -sublattice magnetizations, can be either parallel or antiparallel depending on the signs of K_B and K_A . This

naturally explains why some rare-earth orthoferrites and orthochromates (such as NdFeO_3) have a compensation temperature while others (such as GdFeO_3) do not.⁴²

IV. CONCLUSION

In summary, we have discussed a trilinear atomistic coupling [Eqs. (1) and (2)] involving magnetic moments of the R and M cations and the oxygen octahedral tiltings in RMO_3 perovskites. This energy term naturally explains the existence and properties of the net magnetization associated to the R sublattice in rare-earth orthoferrites and orthochromates. Our theory thus unveils the magnetostructural origin of the *effective magnetic field* acting on the R spins. Considered in combination with another model for the magnetization of the M sublattice [Eqs. (4) and (5)], our theory also explains why some RFeO_3 and RCrO_3 compounds adopt a compensation temperature while others do not. Note that the material-dependency of Eqs (1), (2), (4) and (5) is reflected in the values of the K_A and K_B parameters and that a typical magnitude of such parameters is of the order of $2 \times 10^{-6} \text{ a.u.}/(\mu_B^2 \text{ rad})$, as found for K_B in BiFeO_3 .³⁹ Moreover, taking advantage of the presently determined analytical form of these equations, along with the experimental data on magnetic moments and compensation temperature in various RMO_3 materials, should allow to extract the precise value of K_A and K_B in these systems.

It is important to note that the atomistic coupling discussed here is universal, i.e., it is present in *all* ABO_3 perovskites with magnetic A and B cations. Further, it involves the structural distortion (i.e., rotations of the O_6 octahedra) that is most common in perovskite phases. Hence, beyond ferrites and chromites, our finding is likely to be relevant to explain related or original effects in other compounds, such as manganites, nickelates, etc. Moreover, Eqs (5) and (6) may also be relevant to the appearance of a spontaneous electrical polarization in some orthoferrites and orthochromates,^{3,4,8–10} since Ref. 10 suggested that such polarization can only occur if the B sublattice exhibits a magnetization and our Eqs. (5) and (6) provide the microscopic origin of this latter magnetization. We thus hope that this work will contribute to improve our understanding of these complex systems, and eventually guide the design of functional materials with engineered magnetostructural properties.

This work was supported by the National Natural Science Foundation of China under Grants Nos. 51332006 and 11274270 (X.M.C.), the NSF grant DMR-1066158 (L.B.), FNR Luxembourg Grants FNR/P12/4853155/Kreisel (J.I.) and INTER/MOBILITY/15/9890527 GREENOX (L.B. and J.I.), and MINECO-Spain Grant MAT2013-40581-P (J.I.). We also thank Eric Bousquet for providing us with his review on non-collinear magnetism in multiferroic materials,² before its publication.

- ¹ R.L. White, *J. Appl. Phys.* **40**, 1061-1069 (1969).
- ² E. Bousquet and A. Cano, *J. Phys. Condens. Matt.* (in press).
- ³ Y. Tokunaga, N. Furukawa, H. Sakai, Y. Taguchi, T.-H. Arima and Y. Tokura, *Nat. Mater.* **8**, 558 (2009).
- ⁴ Y. Tokunaga, S. Iguchi, T. Arima and Y. Tokura, *Phys. Rev. Lett.* **101**, 097205 (2008).
- ⁵ A. Kirilyuk, A. V. Kimel and T. Rasing, *Rev. Mod. Phys.* **82**, 2731 (2010).
- ⁶ S. Artyukhin, M. Mostovoy, N. P. Jensen, D. Le, K. Prokes, V. G. de Paula, H. N. Bordallo, A. Maljuk, S. Landsgesell, H. Ryll, B. Klemke, S. Paeckel, K. Kiefer, K. Lefmann, L. T. Kuhn and D. N. Argyriou, *Nat. Mater.* **11**, 694 (2012).
- ⁷ Y. Tokunaga, Y. Taguchi, T.-H. Arima and Y. Tokura, *Nat. Phys.* **8**, 838 (2012).
- ⁸ J.-H. Lee, Y. K. Jeong, J. H. Park, M.-A. Oak, H. M. Jang, J. Y. Son and J. F. Scott, *Phys. Rev. Lett.* **107**, 117201 (2011).
- ⁹ H. J. Zhao, Y. Yang, W. Ren, A.-J. Mao, X. M. Chen and L. Bellaiche, *J. Phys.: Cond. Mat.* **26**, 472201 (2014).
- ¹⁰ B. Rajeswaran, D. I. Khomskii, A. K. Zvezdin, C. N. R. Rao and A. Sundaresan, *Phys. Rev. B* **86**, 214409 (2012).
- ¹¹ K. P. Belov, A. M. Kadomtseva, T.M. Ledneva, T. L.Ovchinnikova and V. A. Timofeeva, *JETP Lett.* **2**, 161 (1965).
- ¹² V. N. Derkachenko, A. M. Kadomtseva, V. A. Timofeeva, and V. A. Khokhlov, *JETP Lett.* **20**, 104 (1974).
- ¹³ B. Rajeswaran, D. Sanyal, M. Chakrabarti, Y. Sundarayya, A. Sundaresan and C. N. R. Rao, *EPL* **101**, 17001 (2013).
- ¹⁴ T. Yamaguchi and K. Tsushima, *Phys. Rev. B* **8**, 5187 (1973).
- ¹⁵ H. J. Zhao, W. Ren, Y. Yang, X. M. Chen and L. Bellaiche, *J. Phys.: Cond. Mat.* **25**, 466002 (2013).
- ¹⁶ H. J. Zhao, W. Ren, X. M. Chen and L. Bellaiche, *J. Phys.: Cond. Mat.* **25**, 385604 (2013).
- ¹⁷ L. Bellaiche, Z. Gui, and I.A. Kornev, *J. Phys.: Condens. Matter* **24**, 312201 (2012).
- ¹⁸ Y. Yang, J. Íñiguez, A.-J. Mao, and L. Bellaiche, *Phys. Rev. Lett.* **112**, 057202 (2014).
- ¹⁹ G. Kresse, and D. Joubert, *Phys. Rev. B* **59**, 1758 (1999).
- ²⁰ S. L. Dudarev, G. A. Botton, S. Y. Savrasov, C. J. Humphreys and A. P. Sutton, *Phys. Rev. B* **57**, 1505 (1998).
- ²¹ J. P. Perdew, J. A. Chevary, S. H. Vosko, K.r A. Jackson, M. R. Pederson, D. J. Singh and C. Fiolhais, *Phys. Rev. B* **46**, 6671 (1992).
- ²² A. Stroppa, M. Marsman, G. Kresse and S. Picozzi, *New J. Phys.* **12**, 093026 (2010).
- ²³ E.F. Bertaut, *Magnetism Vol 3* (Academic, New York, 1963).
- ²⁴ I.A. Kornev, L. Bellaiche, P.E. Janolin, B. Dkhil and E. Suard, *Phys. Rev. Lett.* **97**, 157601 (2006).
- ²⁵ A.M. Glazer, *Acta Crystallogr. Sect. A* **31**, 756 (1975).
- ²⁶ H. Shen, Z. Cheng, F. Hong, J. Xu, S. Yuan, S. Cao and X. Wang, *Appl. Phys. Lett.* **103**, 192404 (2013).
- ²⁷ S. J. Yuan, W. Ren, F. Hong, Y. B. Wang, J. C. Zhang, L. Bellaiche, S. X. Cao and G. Cao, *Phys. Rev. B* **87**, 184405 (2013).
- ²⁸ Y. Cao, S. Cao, W. Ren, Z. Feng, S. Yuan, B. Kang, B. Lu and J. Zhang, *Appl. Phys. Lett.* **104**, 232405 (2014).
- ²⁹ L. G. Marshall, J.-G. Cheng, J.-S. Zhou, J. B. Goodenough, J.-Q. Yan and D. G. Mandrus, *Phys. Rev. B* **86**, 064417 (2012).
- ³⁰ R. Shukla, A. K. Bera, S. M. Yusuf, S. K. Deshpande, A. K. Tyagi, W. Hermes, M. Eul and R. Pottgen, *The Journal of Physical Chemistry C* **113**, 12663 (2009).
- ³¹ S. Lei, L. Liu, C. Wang, C. Wang, D. Guo, S. Zeng, B. Cheng, Y. Xiao and L. Zhou, *J. Mater. Chem. A* —bf **1**, 11982 (2013).
- ³² K. Yoshii, *Journal of Solid State Chemistry* **159**, 204 (2001).
- ³³ N. Shamir, H. Shaked and S. Shtrikman, *Phys. Rev. B* **24**, 6642 (1981).
- ³⁴ K. Yoshii, *Materials Research Bulletin* **47**, 3243 (2012).
- ³⁵ Y. Su, J. Zhang, Z. Feng, L. Li, B. Li, Y. Zhou, Z. Chen and S. Cao, *J. Appl. Phys.* **108**, 013905 (2010).
- ³⁶ L. T. Tsymbal, Ya. B. Bazaliy, V. N. Derkachenko, V. I. Kamenev, G. N. Kakazei, F. J. Palomares and P. E. Wigen, *J. Appl. Phys.* **101**, 123919 (2007).
- ³⁷ K. Tsushima, I. Takemura and S. Osaka, *Solid State Communications* **7**, 71 (1969).
- ³⁸ Let us, e.g., choose a spin configuration for which the predominant magnetic ordering of the M ions is of G-type and along x . The first term of Eq. (5) automatically implies the existence of a (weak) magnetization of the M ions being directed along z (since ω_R is parallel to y in the $Pbnm$ structure), while its third term gives rise to a (weak) A-type vector of the M -sublattice being oriented along y (since ω_M is along z). In other words, one gets (G_x , A_y , F_z) for the magnetic ordering of the M -sublattice, which is precisely the Γ_4 spin structure indicated in Table I and which is very common in $RFeO_3$ and $RCrO_3$ compounds¹. (Note that there is no C-type antiferromagnetism associated to the Γ_4 configuration because the second and fourth terms of Eq. (5) vanish, as a result of the fact that ω_M and \mathbf{F} are parallel to each other and ω_R and \mathbf{A} are collinear.) Similarly, the (F_x , C_y , G_z) ordering inherent to the magnetic Γ_2 structure of Table I is easily understood by Eq. (5) when starting with a predominant G-type ordering along z : its $(\omega_R \times \mathbf{G}) \cdot \mathbf{F}$ term provides a magnetization of the M -sublattice along x , which in turn induces a C-type ordering along y because of the $(\omega_M \times \mathbf{C}) \cdot \mathbf{F}$ term. Note that both $\omega_M \times \mathbf{G}$ and $\omega_R \times \mathbf{C}$ vanish in that case, therefore cancelling the third and fourth terms of Eq. (5), which explains why the Γ_2 configuration does not have any A-type AFM.
- ³⁹ D. Albrecht, S. Lisenkov, W. Ren, D. Rahmedov, I. A. Kornev and L. Bellaiche, *Phys. Rev. B* **81**, 140401(R) (2010).
- ⁴⁰ I. Dzyaloshinsky, *J. Phys. Chem. Solids* **4**, 241 (1958).
- ⁴¹ T. Moriya, *Phys. Rev. Letters* **4**, 228 (1960).
- ⁴² Let us emphasize here why performing *ab-initio* calculations at 0K is enough to determine if a RMO_3 compound has a compensation temperature or not. For that, let us start by recalling that it is well known that at high enough temperature (but below the Néel temperature), only the M sublattice adopts a long-range magnetic ordering, including a possible weak magnetization. In other words, there is no magnetization (or other magnetic ordering) associated with the R sublattice at high enough temperature. Now, let us imagine that first-principles calculations are conducted (at 0K), and reveal that the R sublattice has a magneti-

zation that is not only opposite in direction with respect to that of the M ions but is also larger in magnitude. This situation was, in fact, found in Ref. 27, and automatically implies that the magnetization of the R sublattice first happens at a critical temperature (for which the M sublattice is already magnetized) and then grows much faster

than that of the M ions while being opposed to it when the system is cooled down below this critical temperature. As a result, there will be a temperature at which the magnetization of the R ions will exactly cancel that of the M ions. This temperature is the compensation temperature.